Static and Dynamic Scattering of β-Lactoglobulin Aggregates Formed after Heat-Induced Denaturation at pH 2

Pierre Aymard, Taco Nicolai,* and Dominique Durand

Chimie et Physique des Matériaux Polymères, UMR CNRS, Université du Maine, 72085 Le Mans Cedex 9, France

Allan Clark

Unilever Research Colworth, Sharnbrook, Bedford, MK441LQ, U.K.

Received October 29, 1998; Revised Manuscript Received January 27, 1999

ABSTRACT: The structure and internal dynamics of β-lactoglobulin aggregates formed after heat-induced denaturation at pH 2 and different ionic strengths were investigated using light, neutron, and X-ray scattering. Polydisperse aggregates are formed with a rigid rodlike local structure with mass per unit length close to that of a string of β-lactoglobulin monomers but with a somewhat larger diameter. The persistence length decreases with increasing ionic strength from more than 600 nm at 0.013 M to 38 nm at 0.1 M. At ionic strengths of 0.1 and 0.2 M, a self-similar structure with fractal dimensions of 1.8 and 2.0 is seen by using light scattering. The concentration dependence of the static structure factor and the internal dynamics are close to those of flexible linear chains. In contrast, a rigid behavior is observed at lower ionic strength (0.03 and 0.013 M). The persistence length of aggregates formed at 0.013 M is reduced after dilution in 0.1 and 0.2 M ionic strength solvents but remains larger than that of aggregates formed and diluted in 0.1 and 0.2 M. The ionic strength of formation is thus a determining factor for the structure. At pH 2, there is no evidence for a two-step aggregation process as was observed at pH 7.

Introduction

β-Lactoglobulin is a globular whey protein, with molar mass 18 400 g/mol and radius about 2 nm. In aqueous solution, a reversible dimerization occurs of which the extent depends on the genetic variant, pH, concentration, temperature, and degree of screening of the electrostatic repulsions.[1,2] Upon heating above 50 °C, the native structure is partly altered: a decrease in the amount of ordered zones[3−5] and an increase in the exposure of the tryptophan[6] and the free thiol[7] groups have been reported. "Denatured" proteins aggregate and may eventually form gels, of which the opacity,[8] microstructure,[9−12] and rheology[8,10,11] vary, depending on pH, ionic strength, concentration, and heating conditions.

Recently, light (LS), neutron (SANS) and X-ray (SAXS) scattering techniques have been used to characterize heat-induced aggregates formed in different conditions.[13−23] In an earlier publication,[13] using a combination of LS and SANS, we reported that aggregates formed at pH 7 and with 0.1 M added salt had a self-similar structure over length scales ranging from about 10 to several hundred nanometers. Recent measurements using small-angle light scattering have shown that the length scale over which the aggregates have a fractal dimension $df = 2.05$ extends up to several micrometers.[23] Concentration and heating temperature were found to influence only the kinetics of aggregation in the range investigated, and the structure and dynamics of the aggregates were unaffected. We showed that aggregation proceeds through a two-step mechanism, consisting in the formation of small primary particles (radius about 15 nm) followed by their aggregation in large fractal aggregates.[21] This two-step mechanism had been suggested in earlier work[24,25] but had not been fully characterized.

The present study describes the properties of the β-lactoglobulin aggregates formed at pH 2 in different conditions of ionic strength and is motivated by the fact that β-lactoglobulin only bears positive charges at pH 2 (21 per monomer unit), in contrast to the amphoteric behavior at pH 7. Hence, electrostatic interactions between monomers are purely repulsive and can be screened to different extents by the addition of salt. Moreover, at pH 2, transparent aggregate solutions can be obtained, which allows us to study the static and dynamic properties of the aggregates in the semidilute state. Finally, the disulfide interchange which is involved in the aggregation process at pH 7[24−25] is very unlikely to occur here, because the thiol groups are stable at low pH.[26] Native protein solutions have been fully characterized at room temperature in an earlier study.[2]

Materials and Methods

β-Lactoglobulin was obtained from Sigma (ref. L.0130, batch 98F8030) and is a mixture of the genetic variants A and B. The pH and ionic strength were set by the addition of HCl and NaCl. The addition of 200 ppm NaN_3 prevented bacterial growth. The contribution of added HCl and NaN_3 was taken into account when setting the ionic strength. The solutions were dialyzed against the solvent and filtered through 0.1 μm pore size Anotop filters into glass vials. The protein concentrations ranged between 5 and 40 g/L and were measured by UV spectrophotometry at 278 nm using an extinction coefficient of $\epsilon = 0.96$ L cm^{-1} g^{-1}. For the neutron scattering experiments, salt-free protein was directly dissolved in D_2O together with the required amount of salt and DCl.

The protein solutions were put in glass tubes, covered with paraffin oil to prevent evaporation, and placed in a water bath

10.1021/ma981689j CCC: $18.00 © 1999 American Chemical Society
Published on Web 03/26/1999

set at 80 °C (±0.1 °C) for a set time. The aggregation was quenched by rapid cooling to room temperature. Subsequently, the samples were diluted highly before the light scattering experiments to suppress the effects of interaction and multiple scattering. To obtain sufficient contrast, the neutron scattering measurements were done on undiluted samples (40 or 22 g/L). However, dilution of the sample with the lowest ionic strength from 40 to 10 g/L showed that the influence of interactions on the structure factor is small in the q-range covered by the neutron scattering measurements. The diluted samples remained stable at room temperature over a period of months without any detectable further aggregation or break-up of aggregates. Moreover, aggregates formed at pH 2, 0.2 M, and 80 °C did not change in size when reheated at the same temperature in very dilute conditions.

Static (SLS) and dynamic (DLS) light scattering measurements were made using an ALV-5000 multibit multi-τ correlator in combination with a Malvern goniometer and a Spectra Physics argon ion laser operating with vertically polarized light with a wavelength of $\lambda = 488$ nm. The range of scattering wave vectors covered was $3.0 \times 10^{-3} < q < 3.5 \times 10^{-2}$ nm^{-1} with $q = (4\pi n_s/\lambda)\sin(\theta/2)$, n_s and θ being the solvent refractive index and the angle of observation, respectively. The temperature was controlled by a thermostat bath and was set at 20 °C.

Small-angle neutron scattering (SANS) experiments were done in Saclay (France) and in the Rutherford Laboratory (U.K.). The wave vector range covered in these measurements is $7.0 \times 10^{-2} < q < 3$ nm^{-1}.

Small-angle X-ray measurements (SAXS) were made under vacuum using a Philips PW 1730 constant potential generator (Cu−Kα X-rays, wavelength of 0.1543 nm), a Kratky camera, an INEL LPS 50 position-sensitive detector, associated electronics, and a Varro Silena multichannel analyzer. The q-range covered in these measurements is $0.15 < q < 4$ nm^{-1}. Raw data were corrected for the background scattering and normalized by the concentration and the exposure time. No correction was made for slit-smearing effects.

Electron micrographs of β-lactoglobulin aggregates were obtained by negative staining. A drop of dilute solution of aggregates was placed onto a carbon support film on a copper grid. The grid was washed with several drops of methylamine tungstate and blotted dry. Grids were then examined in a JEOL 1200 EX transmission electron microscope (TEM) operating at 80 KV.

Data Analysis. Solutions of aggregated β-lactoglobulin contain a certain amount of residual nonaggregated protein which decreases with increasing heating time. As we are interested in the structure of the aggregates, we need to subtract the scattering by nonaggregated β-lactoglobulin from the total scattering (I_{tot}). This can be done because DLS shows that the size distribution of the aggregates is well separated from that of native protein (see below). From DLS, the relaxation time distributions of nonaggregated and aggregated β-lactoglobulin are easily distinguished (see e.g., Figure 8b). The relative amplitude of each distribution is proportional to the relative scattering intensity. The scattering of aggregates (I_{ag}) is given as $I_{ag} = A_{ag}(I_{tot} - I_{sol})$, where I_{sol} is the solvent scattering and A_{ag} is the relative amplitude of the relaxation time distribution corresponding to the aggregates.

I_{ag} is proportional to the concentration (C_{ag}), the weight average molar mass (M_w), and the z-average structure factor [$S_z(q)$] of the aggregates: $I_{ag} = KC_{ag}M_wS_z(q)$, where K is a constant which depends on the experimental setup and the refractive index increment of β-lactoglobulin. For highly diluted samples, interaction between particles can be neglected, and $S_z(q)$ is equal to the z-average particle structure factor. The concentration of the aggregates is the total protein concentration minus the concentration of nonaggregated β-lactoglobulin. To measure the latter, we dilute the aggregates formed at pH 2 in a solvent at pH 7, which provokes their precipitation. We confirmed with DLS that the supernatant only contains nonaggregated proteins, which concentration can be deduced from the UV absorbance at 278 nm. The constant K is the same for monomeric and aggregated β-lactoglobulins,

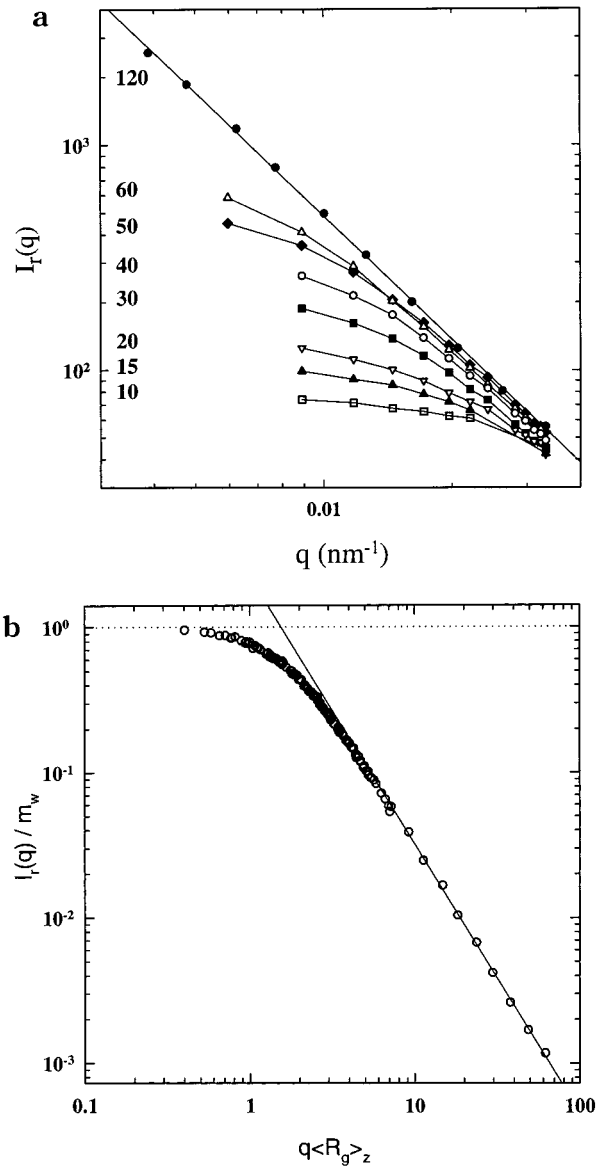

Figure 1. (a) Scattering wave vector dependence of the relative excess intensity of light scattered by dilute solutions of aggregates formed after different times of heating at 80 °C, pH 2, ionic strength 0.1 M, and $C = 22$ g/L. The heating times in minutes are indicated in the figure. The straight line through the data at 120 min has slope −1.82. (b) Same data as in part a with I_r normalized by the weight average aggregation number and q by the z-average radius of gyration.

which means that if we normalize I_{ag} by the scattering of monomeric β-lactoglobulin ($I_m = KC_mM_m$) at the same concentration ($C_m = C_{ag}$) we obtain the relative intensity I_r:

$$I_r = I_{agg}/I_{mon} = m_wS_z(q) \quad (1)$$

Here m_w is the weight average aggregation number of the aggregates. In the light scattering range, the structure factor of monomeric β-lactoglobulin is unity. The advantage of this normalization is that any uncertainty in K and any systematic error in the determination of the concentration is canceled out. In addition, the number of monomers in the aggregate is a more significant parameter than its absolute molar mass.

Results

Overall Structure of β-Lactoglobulin Aggregates at pH 2. Figure 1a shows the relative intensity I_r after

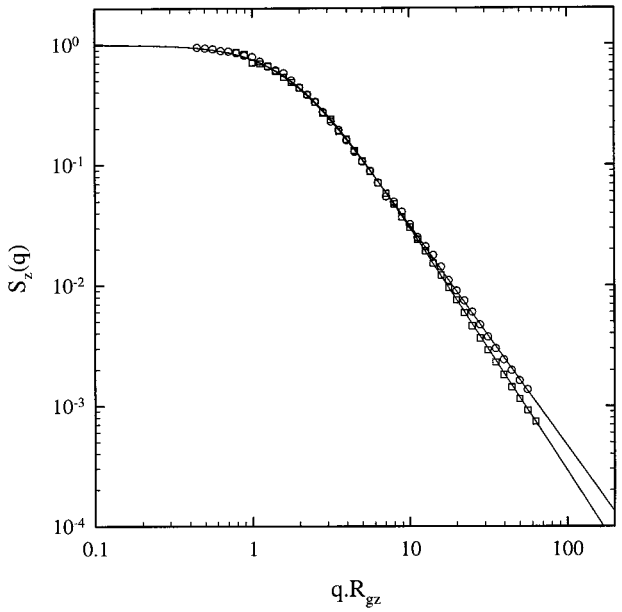

Figure 2. Comparison of the *q*-dependence of the normalized light scattering intensity at ionic strengths 0.1 (circles) and 0.2 M (squares).

different times of heating at 80 °C for 22 g/L β-lactoglobulin at 0.1 M. The solutions were highly diluted so that interactions can be neglected. The value of I_r extrapolated to $q = 0$ represents the weight average aggregation number (m_w), as explained in Materials and Methods. At higher q values, I_r decreases because of the intraparticle interference expressed by the q-dependent particle structure factor $S(q)$.

It is clear that the aggregates grow with increasing heating time and that $S(q)$ becomes more q-dependent. At heating times larger than 120 min we only measure the internal structure independent of the overall size of the particles. $S(q)$ has a power law dependence on q over the whole accessible q-range which demonstrates that the aggregates have a fractal structure. For fractal objects,

$$S_z(q) \propto q^{-df} \quad qR_{gz} \gg 1 \tag{2}$$

where R_{gz} is the z-average radius of gyration. We can superimpose the data measured at different heating times by normalizing the vertical axis with m_w and the horizontal axis with R_{gz}; see Figure 1b. The data superimpose very well within the experimental error of the individual measurements, which implies that the structure and the size distribution of the aggregates do not change significantly with heating time. The master curve shown in Figure 1b represents the z-average static structure factor of the aggregates over a much larger range of qR_{gz} than could be accessed by measurements on a single solution.

An analogous behavior is observed at ionic strength 0.2 M and β-lactoglobulin concentration 5 g/L. The structure factors obtained at 0.1 and 0.2 M are the same for $qR_{gz} < 10$ but have a different final slope at large qR_{gz}; see Figure 2. The shape of the structure factor is determined by the molar mass distribution and the structure of the individual aggregates. A reasonable assumption is that the amount of aggregates with aggregation number m, $N(m)$, has a power law dependence on m with an exponential cutoff at a characteristic aggregation number (m^*) proportional to the z-average aggregation number:

$$N(m) \propto m^{-\mu} \exp(-m/m^*) \tag{3}$$

where μ is the polydispersity exponent. This assumption is based on theory and computer simulations of particle aggregation.[37] For particles with a fractal structure the pair correlation function can be written as[22]

$$g(r) \propto r^{(df-3)} f(r/R_g) \tag{4}$$

where $f(r/R_g)$ is a cutoff function at R_g. The structure factor of an aggregate is given by the Fourier transform of $g(r)$:

$$S(q) = \frac{1}{m_w} \int_0^\infty g(r) 4\pi r^2 \frac{\sin(qr)}{qr}\, dr \tag{5}$$

The z-average structure factor can be calculated if we know N(m):

$$S_z(q) = \frac{\int m^2 N(m) S(q)}{\int m^2 N(m)} \tag{6}$$

To compare the experimental results with eq 6, we need an expression for $f(r/R_g)$. A stretched exponential cutoff function ($\exp[-(r/R_g)^\gamma]$) allows for a variation of the sharpness of the cutoff. The solid lines in Figure 2 show the results of nonlinear least-squares fits to eq 6 with $\gamma = 2.2$, $\mu = 1.1$ at 0.1 M and $\gamma = 1.7$, $\mu = 1.4$ at 0.2 M. The values of μ are in agreement with independent determinations using DLS; see below. For more details, see Aymard et al.[23] In the fit, the value of df was fixed at the value obtained from a linear least-squares fit to the q-dependence of very large aggregates that did not show significant curvature: $df = 1.82 \pm 0.03$ at 0.1 M and $df = 2.02 \pm 0.02$ at 0.2 M (error bars represent 95% confidence interval). The results are consistent with the variation of the radius of gyration with the aggregation number: $m_w = 0.053 R_{gz}^{1.8}$ at 0.1 M and $m_w = 0.035 R_{gz}^{2.0}$ at 0.2 M.[23] The model presented here describes the data within the experimental error. The difference between the fractal dimensions at 0.2 and 0.1 M could be due to stronger repulsive electrostatic interactions in the latter case. This is equivalent to larger excluded-volume interactions. Excluded-volume interactions swell the particles and consequently decrease the fractal dimension.

A qualitatively different behavior is observed at lower ionic strengths (0.013 and 0.03 M). As shown below, the rate of decrease of monomers is much slower than at 0.1 and 0.2 M, so that prolonged heating at 80 °C is necessary to form aggregates. However, this leads to partial precipitation of the aggregates, i.e., the formation of particles of several millimeters that can be removed easily by mild centrifugation. Placed under an optical microscope with polarized light, the particles showed amorphous and crystalline domains. The formation of macroscopic dense particles is unexpected because at low ionic strength interactions are strongly repulsive.[2] The scattering from the supernatant is low but reveals the presence of large soluble aggregates ($R_{gz} > 1$ μm). The superposition procedure described above could not be applied here, as R_{gz} and m_w could not be measured. Attempts to reduce the heating time were not more successful because as soon as the scattering from the

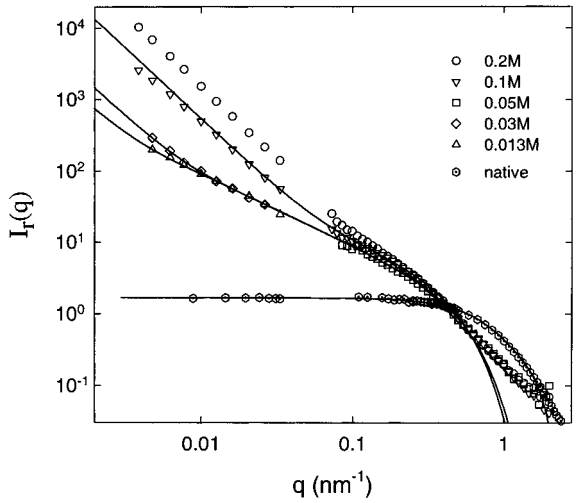

Figure 3. Scattering wave vector dependence of the relative excess intensity scattered by dilute solutions of very large aggregates formed upon heating at 80 °C, pH 2, and different ionic strengths indicated in the figure. The data at $q < 0.04$ nm^{-1} are from light scattering, and the data at $q > 0.07$ nm^{-1} are from neutron scattering. For comparison, we also show the results for native β-lactoglobulin. The solid lines represent model fits discussed in the text.

aggregates was significant we observed $qR_{gz} \gg 1$ over the whole accessible q-range, even if more than 90% of the protein remained nonaggregated. Repeated measurements showed that, because of the partial demixing, the concentration of aggregates C_{agg} (and therefore the relative intensity I_r) could not be estimated accurately for 0.03 and 0.013 M. However, the q-dependence of I_r was reproducible and showed a power law with an exponent close to -1, typical for rigid rodlike structures; see below.

Internal Structure of β-Lactoglobulin Aggregates at pH 2. The local structure of the aggregates was investigated using small-angle neutron scattering and X-ray scattering. To obtain sufficient contrast, the neutron scattering measurements were made on aggregates grown in D_2O. Although the aggregation process is slower in D_2O, no significant difference in structure was observed on the length scale probed by light scattering. We did not measure the absolute neutron scattering intensity directly but instead used the fact that I_r of native β-lactoglobulin is the same for neutron and light scattering in the q-range where it is q-independent; see Figure 3. Neutron scattering results from solutions containing aggregates were normalized by the same factor.

Figure 3 shows the q-dependence of I_r of very large aggregates, i.e., $qR_{gz} \gg 1$ even at the smallest q used in the experiment. The results were obtained from a combination of neutron and light scattering measurements at different ionic strengths. The amount of residual nonaggregated proteins is negligible for these samples. As we did not dialyze the D_2O solutions, the lowest accessible ionic strength for neutron scattering measurements (0.05 M) was imposed by the adjustment of the pH by adding DCl. The combined use of light and neutron scattering gives access to the internal structure of the aggregates over distance scales of nearly 3 orders of magnitude. As mentioned above we could not precisely determine the aggregate concentrations at 0.0013 and 0.03 M. Therefore we adjusted the vertical position the data at these ionic strengths, assuming that they have the same local structure as at 0.05 M; see below.

For comparison, we also show the results for native β-lactoglobulin. The structure of the native proteins is compatible with that of a sphere of radius 1.85 nm which is present as a mixture of monomers and dimers; see solid line through the data. The amount of dimers depends on the ionic strength, pH, temperature, and concentration[2] and is 67% w/w for the sample shown in Figure 3.

Over some q-range $I_r \propto q^{-1}$, which is characteristic for a rigid rodlike structure. The q-range over which $I_r \propto q^{-1}$ decreases with increasing ionic strength and is no longer visible at 0.2 M. At smaller q-values, the q-dependence of I_r is stronger, implying a denser structure. This could be due to flexibility, branching, or both. At larger q-values, the q-dependence is again stronger and is determined by the structure inside the rodlike structure. To describe the q-dependence of I_r quantitatively, we have used the structure factor of large wormlike chains [$S^w(q)$] given by des Cloizeaux.[27] For $qR_{gz} \gg 1$, $S^w(q)$ depends on two parameters: the mass per unit length (m_L) and the persistence length (l_p). For $q \gg l_p$, $S^w(q)$ is equal to the structure factor of a rigid rod so that $I_r \propto q^{-1}$. For $q \ll l_p$ $S^w(q)$ is equal to the structure factor of a Gaussian chain and $I_r \propto q^{-2}$ for $qR_{gz} \gg 1$. We have included the first-order correction for the finite diameter which gives the radius of gyration of the cross-section of the rod R_c:[28]

$$I_r = S^w(q)\exp\left(\frac{-q^2R_c^2}{2}\right) \qquad (7)$$

As I_r is normalized by the scattering of monomeric β-lactoglobulin, m_L is expressed as the number of proteins per unit length. This model does not consider branching, excluded-volume interactions, or the detailed structure on scales smaller than R_c. However, comparison of the data with the wormlike chain model enables us to estimate values for the mass per unit length and the persistence length if the scattering from branching points is small.

The solid lines in Figure 3 represent the results of fits to eq 7. The wormlike chain model gives a good description of the data except at the lowest and highest q values. For the sample at 0.1 M, the wormlike chain model cannot describe the power law q-dependence at small q values because the model assumes that the structure at distance scales larger than l_p is Gaussian, which implies that $df = 2$. In fact, as discussed above, a smaller fractal dimension is observed ($df = 1.82$) which is possibly due to excluded-volume interactions. Another deviation is observed at small length scales ($q > 0.5$ nm^{-1}), as the scattering depends on the way the proteins are connected locally to make up the rodlike structure, which is obviously not taken into account in the model. At these values of q, I_r is independent of the ionic strength and is the same as at pH 7.[20]

The values obtained for the fit parameters allow us to describe more quantitatively the structure for the aggregates formed in different conditions of ionic strengths: the persistence lengths estimated in the fits are 38, 300, and 600 nm at ionic strengths 0.1, 0.03, and 0.013 M, respectively. The value at 0.013 M should be considered as a minimum value, as the deviation from $I_r \propto q^{-1}$ is small. The very large variation in persistence length with ionic strength cannot be attributed to the contribution of electrostatic interaction, as the so-called Debye screening length,[29] which char-

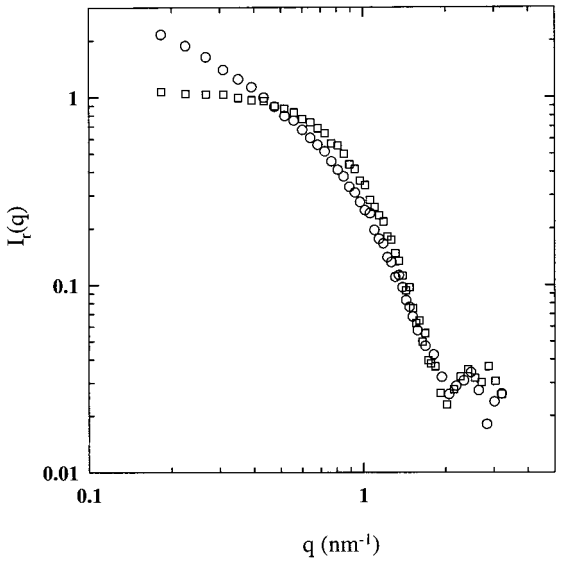

Figure 4. Comparison of the q-dependence of the relative X-ray scattering intensity of native (squares) and aggregated (circles) β-lactoglobulin at pH 2 and 0.1 M.

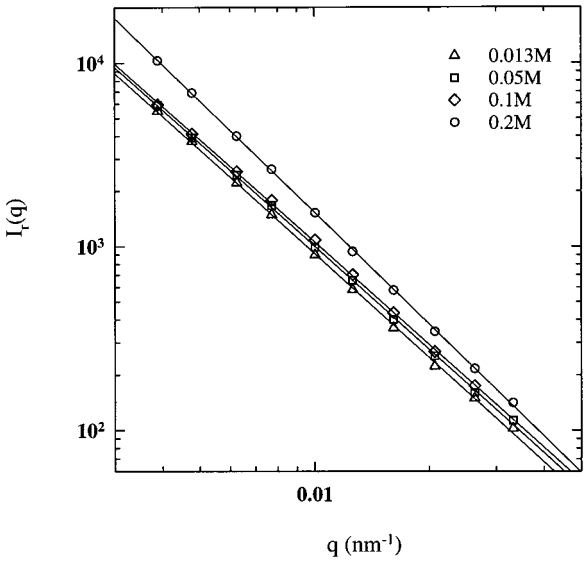

Figure 5. Scattering wave vector dependence of the relative excess intensity of light scattered by dilute solutions of very large aggregates formed at 0.2 M and diluted in the different ionic strengths given in the figure. The solid lines represent linear least-squares fits to the data. The slopes are given in the text.

acterizes the range of the interaction, is only a few nanometers, even at 0.013 M. Concerning R_c and m_L, the fit yields $R_c = 2.3$ nm and $m_L = 0.28$ nm^{-1} at 0.05 M (values used for 0.013 and 0.030 M) and slightly different values at 0.1 M: $R_c = 2.6$ nm and $m_L = 0.33$ nm^{-1}. The observed values of m_L are close to that expected for a string of monomeric β-lactoglobulin molecules: $m_L = 0.27$ nm^{-1}. The values of R_c are higher than the values found for the monomer ($R = 1.85$ nm), and the q-dependence obtained with SANS at $q > 0.5$ nm^{-1} is also significantly different. On the other hand, X-ray scattering shows that for $q > 1.5$ nm^{-1}, i.e., on length scales smaller than the size of a monomer, I_r is close to that of native β-lactoglobulin, which indicates that the size and shape of the proteins are not modified much by the aggregation; see Figure 4.

At ionic strength of 0.2 M, it was not possible to fit the data according to the wormlike model; I_r does not follow the q^{-1} dependence typical for rodlike structures. Possible explanations are a larger flexibility or the influence of scattering by branching points. Note that at 0.1 M a small deviation from the model around $q = 0.15$ nm^{-1}, together with higher values for R_c and m_L compared to those at 0.05 M, could also indicate some branching.

The present results are in agreement with results reported for β-lactoglobulin gels formed at pH 2 using SANS. A rodlike behavior was observed at 0.03 and 0.1 M NaCl, and similar conclusions were drawn concerning the thickness of the strands.[17] However, the distinction between persistence length and fractal dimension was not made, and the gel was assumed to be formed by the rods observed at the local level. The formation of rodlike aggregates at low pH has also been shown by microscopy.[9]

Influence of Electrostatic Interactions on the Internal Structure. As shown above, the structure of the aggregates is highly dependent on the ionic strength. To see to what extent this is controlled by electrostatic repulsions, we diluted large aggregates formed at 0.2 and 0.013 M in solvents of respectively lower and higher ionic strengths and measured the q-dependence of I_r.

Figure 5 shows the limiting q-dependence of aggregates formed at 0.2 M diluted in solvents with the following ionic strengths: 0.2, 0.1, 0.05, and 0.013 M, keeping the pH at 2. The fractal dimension decreases weakly from 2.02 ± 0.02 at 0.2 M to 1.87 ± 0.04 at lower ionic strength. The small decrease of df could be due to repulsive electrostatic interactions that are more important in solvents containing less salt. The total scattering of aggregates formed at 0.2 M remains larger than that of aggregates formed at 0.1 M irrespective of the ionic strength after dilution. This could imply that the local structure of the aggregates formed at 0.2 M is not influenced much by dilution in solvents containing less salt. SANS measurements are needed to verify this point.

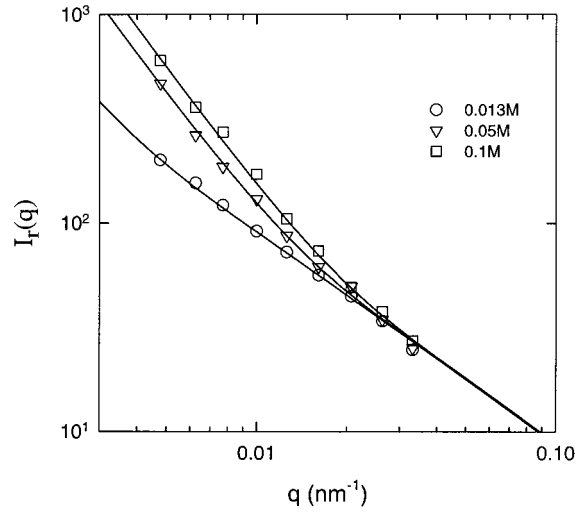

Figure 6. Scattering wave vector dependence of the relative excess intensity of light scattered by dilute solutions of very large aggregates formed at 0.013 M and diluted in the different ionic strengths given in the figure. The solid lines represent model fits discussed in the text.

Figure 6 shows the limiting q-dependence of aggregates formed at 0.013 M and diluted in water at ionic strengths of 0.1, 0.05, and 0.013 M. Dilution in 0.2 M led to partial precipitation of the aggregates. The vertical position of the data at each ionic strength is

established by assuming $m_L = 0.28$ nm^{-1} for all dilutions. The data are compatible with the assumption that the variation is due simply to a decrease of the persistence length with increasing ionic strength. The solid lines in Figure 6 result from fits to eq 2 with l_p equal to 600, 170, and 120 nm at 0.013, 0.05, and 0.1 M, respectively. Nevertheless, the persistence length remains much larger for aggregates formed at 0.013 M and subsequently diluted in 0.1 M (120 nm) than that for aggregates formed and diluted at 0.1 M (38 nm). The results show clearly that the ionic strength conditions at which the aggregates grow are a determining factor for their structure.

The Effect of Progressive Dilution on the Structure Factor. The effect of progressive dilution on the structure factor of solutions containing large β-lactoglobulin aggregates can only be studied for a limited range of conditions. The solution has to be transparent before dilution and should not precipitate upon dilution. The first condition excludes aggregation at 0.2 M which leads to turbid solutions. The second condition excludes the low ionic strengths (0.013 and 0.030 M), which show partial precipitation upon dilution. In addition, the intensity scattered by undiluted solutions at low ionic strength fluctuates slowly in time and is not the same at different positions of the sample. This indicates that the system contains slowly relaxing heterogeneities. Progressive dilutions were therefore carried out at 0.1 M, which yields transparent solutions that do not demix.

Figure 7a shows the q-dependence of the scattered light intensity of a solution containing large aggregates grown at pH 2 and 0.1 M. At the initial concentration, 25 g/L, the q-dependence is rather weak, with an apparent aggregation number, m_a, of 120 and an apparent radius of gyration, R_{ga}, of 80 nm. Upon dilution, the apparent aggregation number and radius of gyration increase. After being diluted by more than a factor of 30, only the internal fractal structure of the aggregates can be observed. Again, a master curve can be obtained by superposition of the data at different concentrations. The resulting structure factor is compared in Figure 7b with the structure factor obtained by measuring highly diluted aggregates of different size as discussed above.

The smaller values of m_a and R_{ga} at higher concentrations are due to interpenetration of aggregates, which leads to screening of interactions and a reduction of the distance over which the positions of monomers are correlated.[22] After dilution, the aggregates disinterpenetrate, which increases the correlation length and thus m_a and R_{ga}. At infinite dilution, the correlation length is proportional to R_{gz}, which is outside the window of observation.

Scaling predictions exist for the concentration dependence of m_a and R_{ga} for semidilute good solvent solutions of linear flexible polymers[30] ($R_{ga} \propto C^{-0.75}$) and of percolating clusters[31] ($R_{ga} \propto C^{-1.7}$). These predictions were shown to be in agreement with experimental results.[32] Using the three available concentrations, we find $R_{ga} \propto C^{-0.7}$ which is compatible with that of linear flexible polymers and excludes the model of percolating clusters.

Dynamic Light Scattering. Figure 8a shows the normalized intensity autocorrelation functions [$g_2(t)$] measured in dilute solutions of aggregates formed at pH 2 and 0.1 M after different periods of heating at 80 °C. Results of SLS on these solution are shown in Figure 1. The correlation functions were analyzed in terms of

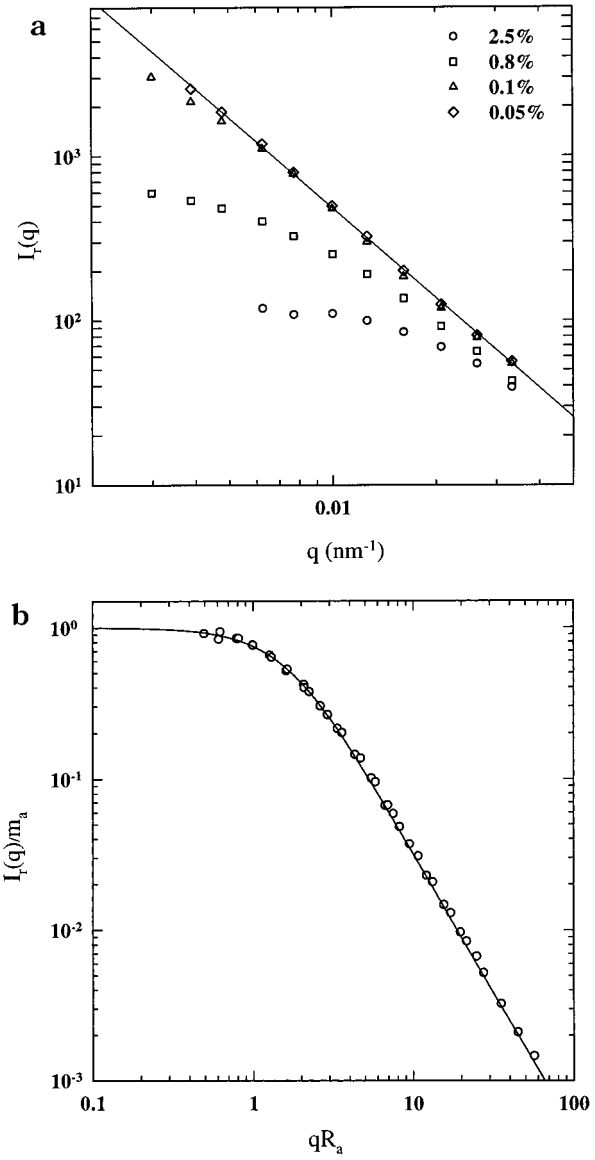

Figure 7. (a) Scattering wave vector dependence of I_r of a solution heated for 2 h at 80 °C, pH 2, ionic strength 0.1 M, and $C = 25$ g/L at different dilutions. The concentrations are indicated in the figure. (b) Same data as in part a with I_r normalized by the apparent aggregation number and q by the apparent radius of gyration. For comparison, we also show the result (solid line) of dilute solutions at different heating times; see Figure 2.

a continuous relaxation time distribution, $A(\tau)$:

$$g_2(t) - 1 = [\int A(\tau)\exp(-t/\tau)\, d\tau]^2 \qquad (8)$$

where we have used the so-called Siegert relation to relate the electric field autocorrelation function to the intensity autocorrelation function.[33] The REPES routine[34] was used to obtain $A(\tau)$ without imposing a specific form. The disadvantage of this method is that single-peaked broad distributions are sometimes falsely represented by a multiple-peaked distribution. For this reason we have also used a combination of a log-normal distribution and the so-called generalized exponential (GEX) distribution.[35] The latter is expressed as

$$A(\tau) = K_n \tau^{p-1} \exp[-(\tau/\tau_g)^s] \qquad (9)$$

where K_n is a normalization constant and p, s, and τ_g

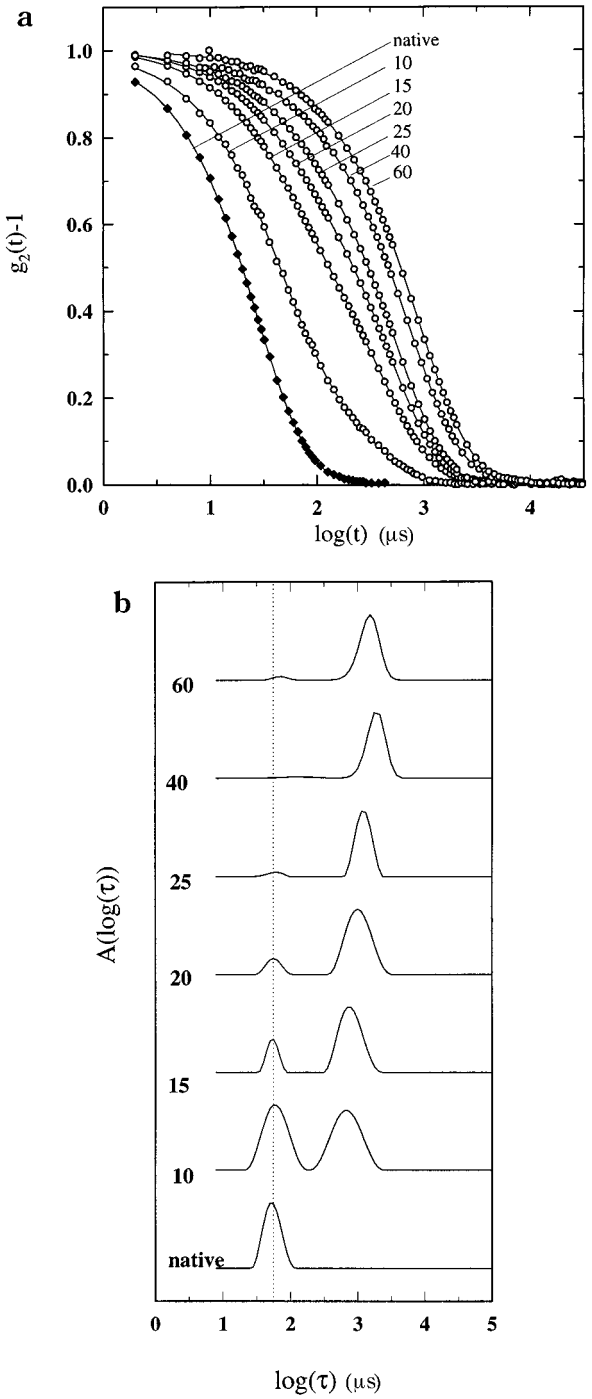

Figure 8. (a) Normalized intensity autocorrelation functions measured in dilute solutions of aggregates formed after different periods of heating at 80 °C, pH 2, 0.1 M, and $C = 22$ g/L. The scattering angle is 50°. The heating times in minutes are given in the figure. The solid lines represent fit results. (b) Relaxation time distributions corresponding to the correlation functions shown in part a.

are fit parameters. The GEX distribution describes a wide range of single-peaked broad distributions.

The data are well-described by both fit procedures; see solid lines in Figure 8a. The corresponding relaxation time distributions are shown in Figure 8b. At relatively short heating times, scattering by nonaggregated β-lactoglobulin cannot be neglected and leads to a peak at short relaxation times. Scattering by aggregates gives a peak at longer relaxation times. Both the relative intensity and the relaxation time of the second peak increase with increasing heating time, because of the growth of the aggregates. The relative amplitude of the slow relaxation mode was used to calculate the q-dependence of I_r shown above. From the scattering by the nonaggregated β-lactoglobulin, one can calculate their concentration, which is in agreement with direct measurements using UV absorption after precipitation of the aggregates. The relaxation time of nonaggregated β-lactoglobulin is q^2-dependent and can be used to calculate the z-average translation diffusion coefficient [$D_z = (q^2\tau)^{-1}$]. The z-average hydrodynamic radius, R_{hz}, can be calculated using the Stokes−Einstein relation:

$$R_{hz} = \frac{kT}{6\pi\eta D_z} \tag{10}$$

where k is Boltzmann's constant, T is the absolute temperature, and η is the solvent viscosity. The hydrodynamic radius of nonaggregated β-lactoglobulin is independent of the heating time and is the same as before heating, which suggests that thermal denaturation at 80 °C is reversible as long as the proteins do not aggregate. The measured value of R_{hz} of native β-lactoglobulin at 20 °C is an average of the dimer and the monomer and thus depends weakly on the concentration and the ionic strength.[2]

After short heating times, the relaxation time of the aggregates is q^2-dependent over the available q-range. At longer heating times, the q-dependence is stronger, and the apparent diffusion coefficient (D_a) increases at larger q-values because of the contribution of internal dynamics. Figure 9a shows the q-dependence of D_a at different heating times. For very large aggregates, we find $D_a \propto q$ over the whole q-range investigated. This dependence is typical for flexible polymers[36] and is consistent with the relatively low value of the persistence length found for the aggregates grown in 0.1 M. The data measured at different heating times were superimposed by normalizing the vertical axis with D_z and the horizontal axis with R_{gz}; see Figure 9b. The data superimpose well within the experimental noise demonstrating that the internal dynamics of the aggregates also are independent of heating time. The results for aggregates grown at ionic strength 0.2 M are very similar. The normalized q-dependence of the apparent diffusion coefficient is the same (see Figure 9b), again showing a fully flexible structure.

If the solution contains large aggregates, the scattering by nonaggregated proteins can be neglected. In this case, the relaxation time distribution measured at $qR_{gz} < 1$ reflects the size distribution of the aggregates as the relaxation time is simply proportional to R_h. We can relate the relaxation time distribution to the molar mass distribution because R_h of fractal aggregates is related to m as $R_h(m) \propto m^{1/d_f}$. Utilizing eq 3, it can be easily shown that the relaxation time distribution is given by eq 9 with $p = df(3 - \mu)$ and $s = df$.[22] The model fits the data very well; see Figure 10. Using for df the values obtained from SLS, we obtain $\mu = 1.2 \pm 0.1$ at 0.1 M and $\mu = 1.4 \pm 0.1$ at 0.2 M. These values are, within experimental error, the same as those obtained from SLS.

DLS data on aggregates formed at ionic strength 0.013 M again show the contribution of residual nonaggregated proteins and aggregates. Also in this case, the relaxation time of the nonaggregated proteins is independent of the heating time. However, the relative

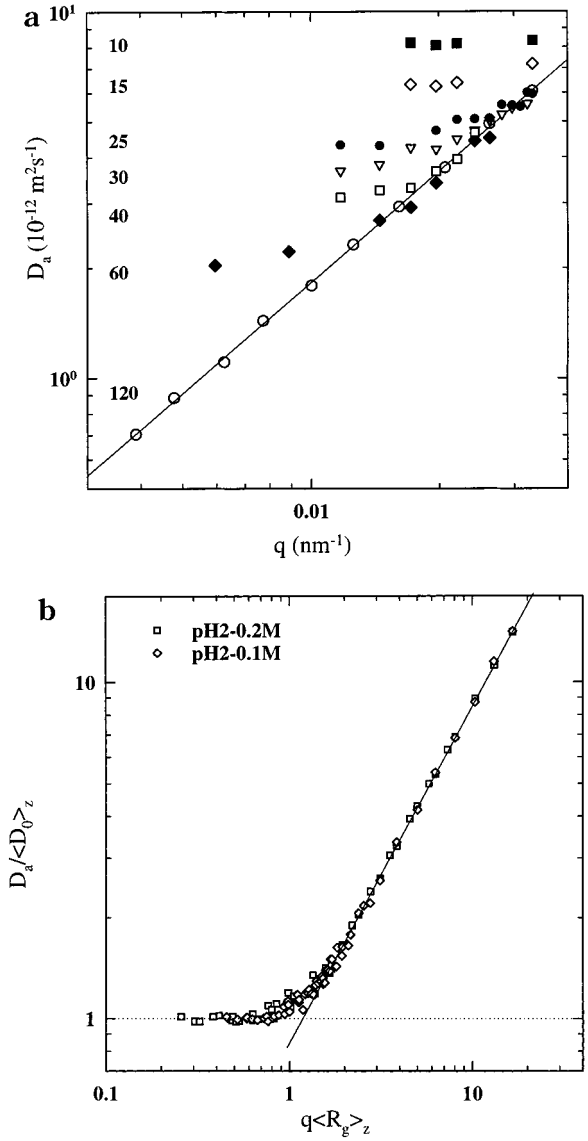

Figure 9. (a) Scattering wave vector dependence of the apparent diffusion coefficient of diluted aggregates formed after different heating times at 80 °C, pH 2, ionic strength 0.1 M, and $C = 22$ g/L. The heating times in minutes are given in the figure. (b) Same data as in part a with D_a normalized by the z-average diffusion coefficient and q by the z-average radius of gyration.

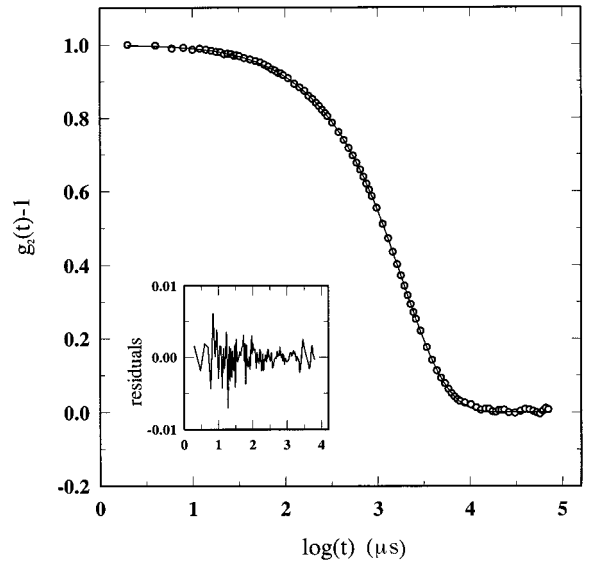

Figure 10. Normalized intensity auto correlation functions measured in a dilute solution of aggregates formed after 30 min heating at 80 °C, pH 2, 0.1 M and $C = 22$ g/L. The scattering angle is 30°. The solid lines represent the fit to the model given in the text. The inset gives the residuals to the fit.

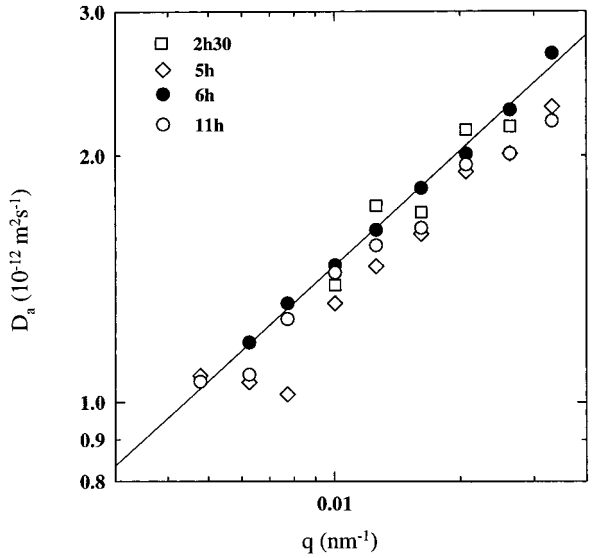

Figure 11. Scattering wave vector dependence of the apparent diffusion coefficient of diluted aggregates formed after different heating times at 80 °C, pH 2, ionic strength 0.013 M, and $C = 5$ g/L. The heating times are given in the figure.

amplitude of the slow mode is not reproducible because of the heterogeneity of the system at this ionic strength and the varying amount of precipitation of aggregates upon dilution. The q-dependence of the apparent diffusion coefficient of the aggregates is independent of the heating time; see Figure 11. SLS results show the formation of long rodlike aggregates, with $qR_g > 1$ over the accessible q-range, so that only their internal structure is measured. Within experimental error, the q-dependence of D_{app} can be fitted to $D_a \propto q^{0.5}$. This dependence is intermediate between that of flexible and rigid particles. An alternative interpretation is that the data are in the crossover regime between a linear dependence on q at small wave vectors and a q-independence at large wave vectors. This interpretation means that the aggregates are flexible at large length scales and rigid at small length scales.

Influence of Electrostatic Interactions on the Internal Dynamics. The apparent diffusion coefficient of larger aggregates formed at 0.2 M is independent of the ionic strength of the solvent in which the aggregates are diluted. This means that the aggregates remain flexible on the length scale probed by light scattering even at 0.013 M. This is compatible with SLS results which showed that the persistence length remains small.

Figure 12 shows the q-dependence of D_a of aggregates formed at 0.013 M and diluted in solvents with ionic strengths 0.05 and 0.1 M. The q-dependence increases with increasing ionic strength and is linear at 0.1 M. The increasing flexibility could mean a decreasing persistence length in accordance with our interpretation of the SLS results.

Discussion

The experimental results indicate that at pH 2 heated β-lactoglobulin forms aggregates with a broad size

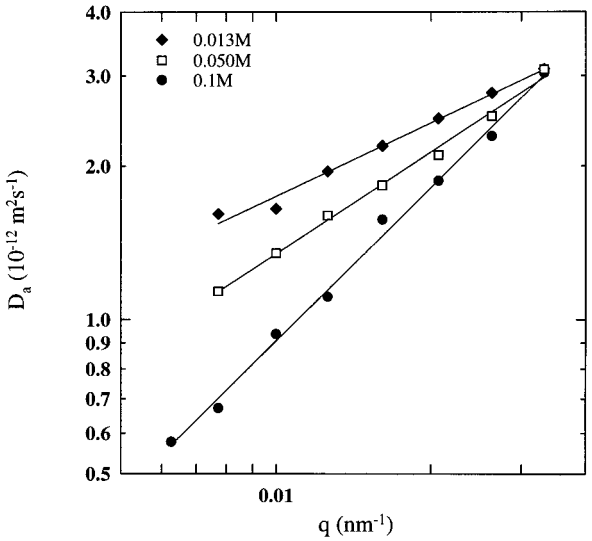

Figure 12. Scattering wave vector dependence of the apparent diffusion coefficient of diluted aggregates formed at 0.013 M and diluted in the different ionic strengths given in the figure. The solid lines represent linear least-squares fits to the data. The slopes are 0.47, 0.66, and 1.00 for the ionic strengths 0.013, 0.05, and 0.1 M, respectively.

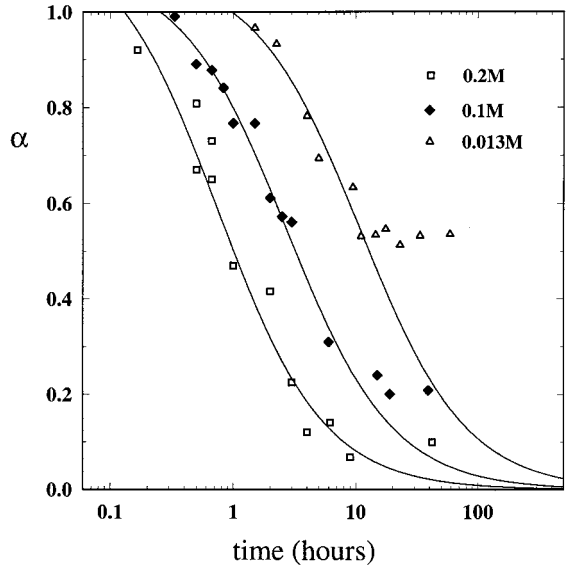

Figure 13. Fraction of nonaggregated β-lactoglobulin as a function of heating time at 80 °C, pH 2, $C = 5$ g/L and the different ionic strengths indicated in the figure

distribution and a structure which depends on the ionic strength. At ionic strengths of 0.1 and 0.2 M, the self-similar structure at large length scales can be probed in the q-range accessible with LS. At 0.030 M, the q-dependence of I_r only shows the beginning of the transition from a local rigid rodlike structure to an more dense overall structure. At 0.013 M, the transition to a denser overall structure can hardly be detected. The mass per unit length in the rigid rodlike domain is close to that of a string of monomeric β-lactoglobulin but with a somewhat larger diameter. We were not able to fit the structure factor at high q-values to any particular shape such as a helix but we can speculate that, at least at the lowest ionic strengths, the local structure is a rigid chain of monomeric β-lactoglobulin with an irregular helical structure. At 0.2 M, an excess of scattering in the persistence domain may suggest some branching. On length scales smaller than the diameter of chain, the structure factor of the aggregates is independent of the ionic strength and similar to that observed at pH 7.[20] All of these observations indicate that the aggregates are essentially wormlike chains with a persistence length that strongly depends on the ionic strength. The large persistence length at low ionic strength cannot be attributed solely to electrostatic interactions, but could be due to specific site binding of the proteins to each other.

Ionic strength not only influences the structure of the aggregates but also governs the rate at which monomers are involved in the formation of aggregates. At the same temperature (80 °C) and concentration (5 g/L), the reaction kinetics are slower than lower ionic strengths (Figure 13). After long heating times, the fraction of nonaggregated proteins stabilizes at a value which increases with decreasing ionic strength. A possible explanation of this feature is that stable aggregates are only formed if the concentration of nonaggregated proteins is larger than a critical value, which depends on the external conditions (e.g., ionic strength or concentration). This explanation is corroborated by the fact that the fraction of nonaggregated proteins stabilizes at a lower value for a solution with a higher protein concentration.

A remarkable feature is that although the kinetics are slower at low ionic strength (0.013 and 0.03 M), some long "fiberlike" aggregates are observed even if the vast majority of the proteins remains nonaggregated. In terms of a nucleation and growth process, we could speculate that, because of the large repulsive interactions between monomers, nucleation is the limiting step. However, once a critical size is reached, the growth process could be relatively fast, which would explain the presence of the very large aggregates. Note that the rate of decrease in monomers was measured at room temperature and that the small aggregates may not be stable to cooling and dilution. Aggregation could possibly become irreversible only if aggregates have reached a critical size of stability.

At higher ionic strengths, electrostatic repulsions are weaker. Possibly, the critical size of stability for the nuclei is smaller, and the nucleation process is no longer the limiting growth step. This may explain why the size of the aggregates is correlated with the fraction of aggregated protein as it is in the case of aggregation at pH 7 and 0.1 M. A more systematic study of the kinetics of the aggregation process is in progress.

The measurements on aggregates grown at a certain ionic strength and diluted in water at other ionic strengths show that the conditions of growth are important. The persistence length of aggregates grown at ionic strength 0.2 M does not strongly increase when diluted at 0.013 M, and the rigid structure formed at 0.013 M is only partly broken by dilution at higher ionic strength. These measurements again indicate the presence of specific protein site binding at low ionic strength, which is partly restructured when electrostatic interactions are screened.

The structure factor contains information about the relative position of the proteins in the aggregate but not about the way they are connected. From scattering measurements, we cannot tell the extent of branching unless the branching points scatter significantly. However, even if branching exists, it only occurs at length scales larger than the persistence length. The fact that

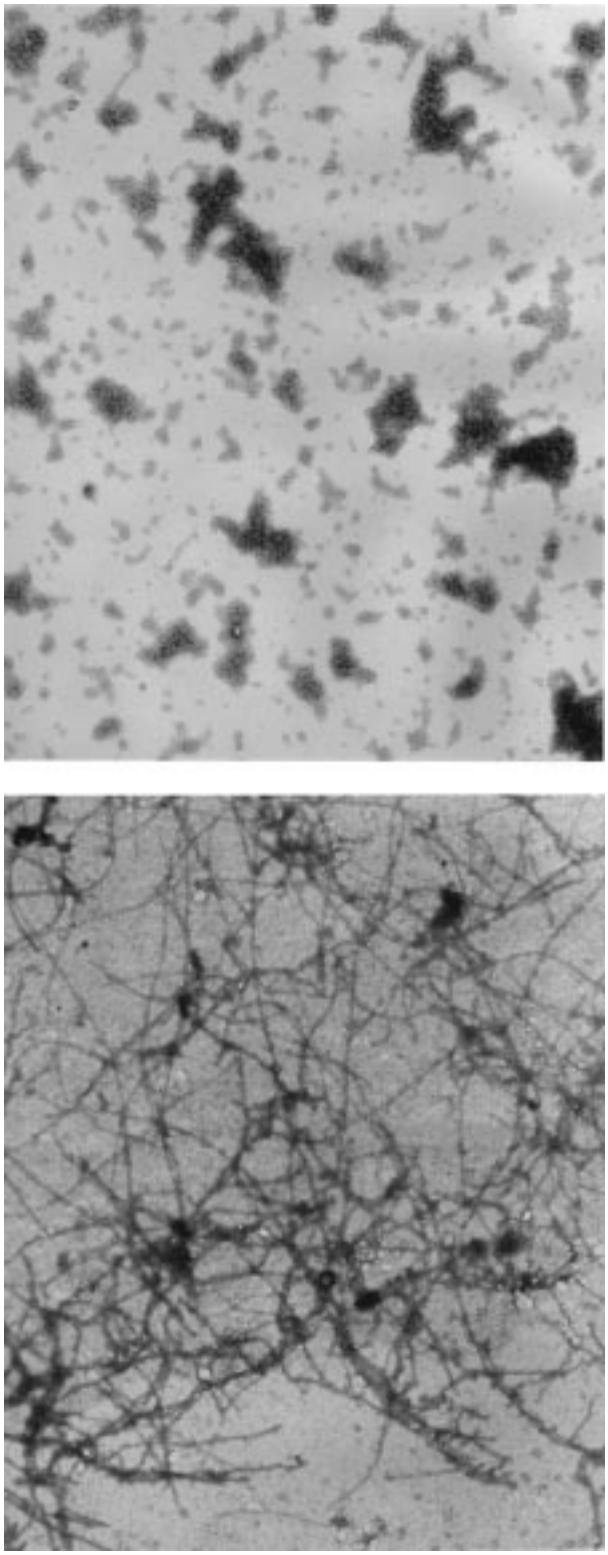

Figure 14. Electron micrographs of aggregates formed upon heating at pH 7 and 0.1 M (top) and pH 2 and 0.03 M (bottom). The magnification is 4×10^4.

the solutions do not flow after long heating periods does not necessarily mean that a three-dimensional cross-linked network exists. At low ionic strength, the system could be more akin to a colloidal particle gel than a rubber. The measurements on progressively diluted samples at 0.1 M resemble those on semidilute solutions of linear flexible chains, indicating that there is little branching at this ionic strength.

At long heating times and low ionic strength, macroscopic structures are formed which contain ordered and disordered domains. It is possible that the ordered domains are due to partial parallel association of the rigid rodlike domains of the aggregates.

The aggregation process at pH 2 is qualitatively different from that at pH 7. Micrographs of aggregates formed at pH 2 and 7 show the difference between the wormlike strings formed at pH 2 and 0.013 M and the denser aggregates formed at pH 7 and 0.1 M; see Figure 14. At pH 2, there is no indication for the two-step growth process mentioned in the Introduction and discussed in Kella and Kinsella.[7] This is not due to discrepancies in charge densities, as globular structures are still observed at pH 7 and very low ionic strength.[21] A more relevant difference is the exchange of disulfide bonds at pH 7, which has been shown to be involved in the first step of the aggregation.[25] The local structure of β-lactoglobulin aggregates appears to depend on the reactivity of the free thiol groups leading to a globular local structure at pH 7 where thiol groups are unstable and a string of monomers at pH 2 where thiol groups are stable. A similar fractal dimension is found for aggregates grown at pH 7 and 0.1 M and at pH 2 and 0.2 M,[20] for which the degree of screening is comparable.[2] The large-scale structure of the aggregates is thus independent of the local chemistry and is governed by the balance between electrostatic interactions and the degree of screening

Acknowledgment. We thank Mr. T. Weaver, Unilever Research Colworth, for doing the TEM. microscopy experiments.

References and Notes

(1) McKenzie, H. A. In *Milk Proteins: Chemistry and Molecular Biology*; Academic Press: New York, 1971; Vol. II.
(2) Aymard, P.; Durand, D.; Nicolai, T. *Int. J. Biol. Macromol.* **1996**, *19*, 213.
(3) Casal, H. L.; Kohler, U.; Mantsch, H. H. *Biochim. Biophys. Acta* **1988**, *957*, 11.
(4) Kaminogawa, S.; Shimizu, M.; Ametani, A. *Biochim. Biophys. Acta* **1988**, *998*, 50.
(5) QI, X. L.; Holt, C.; Mcnulty, D.; Clarke, D. T.; Brownlow, S.; Jones, G. R. *Biochem. J.* **1997**, *324*, 341.
(6) Mills, O. E. *Biochim. Biophys. Acta* **1976**, *434*, 324.
(7) Kella, N. K. D.; Kinsella, J. E. *Int. J. Pept. Protein Res.* **1988**, *32*, 396.
(8) Renard, D.; Lefebvre, J. *Int. J. Biol. Macromol.* **1992**, *5*, 523.
(9) Langton, M.; Hermansson, A. M. *Food Hydrocolloids* **1992**, *6*, 523
(10) Stading, M.; Langton, M.; Hermansson, A. M. *Food Hydrocolloids* **1992**, *6*, 455.
(11) Stading, M.; Langton, M.; Hermansson, A. M. *Food Hydrocolloids* **1993**, *7*, 213.
(12) Boye, J. I.; Ma, C.-Y.; Ismail, A.; Harwalkar, R.; Kalab, M. *J. Agric. Food Chem.* **1997**, *45*, 1608.
(13) Gimel, J. C.; Durand, D.; Nicolai, T. *Macromolecules* **1994**, *257*, 583.
(14) Vreeker, R.; Hoekstra, I. L.; den Boer, D. C.; Agterof, W. G. M. *Food Hydrocolloids* **1992**, *6*, 423.
(15) Griffin, W. G.; Griffin, M. C. A.; Martin, S. R.; Price, J. *J. Chem. Soc., Faraday Trans.* **1993**, *89*, 3395. Griffin, W. G.; Griffin, M. C. A. *J. Chem. Soc., Faraday Trans.* **1993**, *89*, 2879.
(16) Hagiwari, T.; Kumagai, H.; Nakamuri, K. *Biosci. Biotechnol. Biochem.* **1996**, *60*, 1757.
(17) Renard, D.; Axelos, M. A. V.; Lefebvre, J. In *Food Macromolecules and Colloids*; Dickinson, E., Lorient, D., Eds.; Royal Society of Chemistry: Cambridge, U.K., **1995**.
(18) Roefs, S. P. F. M.; de Kruif, C. G. *Eur. J. Biochem.* **1994**, *226*, 883.
(19) Renard, D.; Axelos, M. A. V.; Boue, F.; Lefebvre, J. *Biopolymers* **1995**, *39*, 149.

(20) Aymard, P.; Nicolai, T.; Durand, D. *Int. J. Polym. Anal. Charact.* **1996**, *2*, 115.
(21) Aymard, P.; Gimel, J. C.; Nicolai, T.; Durand, D. *J. Chim. Phys.* **1996**, *93*, 987.
(22) Nicolai, T.; Durand, D.; Gimel, J. C. In *Light Scattering. Principles and Developments*; Brown, W., Ed.; Clarendon Press: Oxford, 1996.
(23) Aymard, P.; Durand, D.; Nicolai, T.; Gimel, J. C. *Fractals* **1997**, *5*, 23.
(24) Sawyer, W. H. *J. Dairy Sci.* **1968**, *51*, 323.
(25) Shimada, K.; Cheftel, J. C. *J. Agric. Food Chem.* **1989**, *37*, 161.
(26) Harwalkar, V. R.; Kalab, M. *Milchwissenschaften.* **1985**, *40 (11)*, 665.
(27) Des Cloizeaux, J. *Macromolecules* **1973**, *6*, 403.
(28) Porod, G. In *Small Angle X-ray Scattering*; Glatter, O., Kratky, O., Eds.; Academic Press: Oxford, 1996.
(29) Sedlak, M. In *Light Scattering. Principles and Developments*, Brown, W., Ed.; Clarendon Press: Oxford, 1996.
(30) de Gennes, P. G. In *Scaling Concepts in Polymer Physics*; Cornell University Press: London, 1979.
(31) Daoud, M.; Leibler, L. *Macromolecules* **1988**, *21*, 1497.
(32) Brown, W.; Nicolai, T. *Colloid Polym. Sci.* **1990**, *268*, 977. Lesturgeon, V.; Nicolai, T.; Durand, D. *Europhys. Lett.* **1996**, *35*, 573.
(33) Berne, B.; Pecora, R. In *Dynamic Light Scattering*; Brown, W., Ed.; Oxford University Press: Oxford, U.K., 1993.
(34) Stepanek, P. In *Dynamic Light Scattering*, Brown, W., Ed.; Oxford University Press: Oxford, U.K., 1993.
(35) Nicolai, T.; Gimel, J. C.; Johnsen, R. *J. Phys. II* **1996**, *6*, 697.
(36) Schaefer, D. W.; Han, C. C. In *Dynamic Light Scattering*; Pecora, R., Ed.; Plenum Press: New York, 1985.
(37) Meakin, P. *Phys. Scr.* **1992**, *46*, 295

MA981689J